Hindawi
Advances in Condensed Matter Physics
Volume 2018, Article ID 5045427, 7 pages
https://doi.org/10.1155/2018/5045427

Research Article

Effect of Silver Nanowire Plasmons on Graphene Oxide Coatings Reduction for Highly Transparent Electrodes

Xingzhen Yan, Lu Zhou, Xuefeng Chu, Huan Wang, Fan Yang, Chao Wang, Yaodan Chi, and Xiaotian Yang

Jilin Provincial Key Laboratory of Architectural Electricity & Comprehensive Energy Saving, Jilin Jianzhu University, 5088 Xincheng Street, Changchun 130118, China

Correspondence should be addressed to Xingzhen Yan; yanxz660@nenu.edu.cn and Xiaotian Yang; hanyxt@163.com

Received 16 May 2018; Revised 12 July 2018; Accepted 7 August 2018; Published 2 September 2018

Academic Editor: Jan A. Jung

We prepared transparent conducting composite electrodes composed of silver nanowires (Ag NWs) and reduced graphene oxide (r-GO). We present a simple approach to welding the cross-positions of the Ag NWs by applying pressure at a relatively low temperature (100°C). We examined the Ag NWs/r-GO composite films in terms of their transmission, conductivity, and stability. The plasmonic features of the Ag NWs were used to assist the ultraviolet (UV) light-induced reduction of the GO coating. The r-GO coatings used to form Ag NWs/r-GO composite structures increased the conductivity of the film by providing more efficient electron conductive pathways. The G/D intensity ratios of the GO and r-GO produced by the UV light-induced method without and with Ag NWs were 0.95, 1.01, and 1.04, respectively. The lowest sheet resistance of the composite films was 7 ohm/sq with approximately 82% transparency in the visible spectrum region. No degradation of the films was observed after 2 months. This excellent environmental stability might facilitate applications of Ag NWs/r-GO composite films in optoelectronic devices.

1. Introduction

Transparent conductive films (TCFs) have become the electrode of choice for many optoelectronic devices in recent years, including transparent displays, organic light-emitting diodes, touch-panel screens, and solar cells [1–3]. For these purposes, TCFs have been widely developed. Currently, indium tin oxide (ITO) is commonly used in a variety of applications [4, 5]. However, its brittleness and high costs have limited its applications in optoelectronic devices [6–8]. To overcome the shortcomings of ITO, currently considered alternative material systems for TCFs include one-dimensional (1D) random networks of metallic nanowires [9–12], carbon nanotubes [3, 13, 14], and 2D graphene films [15–17]. Among these alternatives material systems, random Ag NW networks show TCFs performances very close to that of ITO and are regarded as a promising candidate material to replace ITO [10, 18, 19]. The formation of random Ag NW networks can be achieved by simple and low-cost solution processing methods, such as drop casting, spin coating, rod coating, and air spraying. Furthermore, Ag NW networks show remarkably high TCFs performance in terms of conductivity and transparency. Large open areas, of the order of several μm^2, between the wires provide optical transparency and charge transport occur along the wires. The Ag NW networks in the composite electrode can promote electron collection and injection in regions farther from the metal probe because the Ag NWs can act as a broad-range collector and injector due to their length, which will improve the efficiency of optoelectronic devices [20]. However, there are still several problems associated with high contact resistance caused by loose contact among NW-NW, poor adhesion to substrates, and instability in the harsh environments that must be addressed before practical applications of Ag NW networks [21–24].

Currently, many groups have proposed methods for fabricating Ag NWs-polymer composite films to resolve the shortcomings of pure Ag NW networks [25, 26]. However, conducting polymers such as poly3,4-ethylenedioxythiophene have been shown to promote degradation in organic optoelectronic devices and severely limit device lifetimes. The

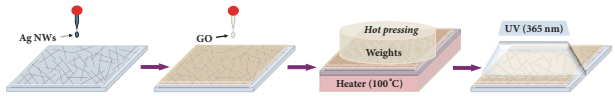

Figure 1: Schematic diagram of the fabrication procedure for Ag NWs/r-GO composite electrode.

poor conductivity and low stability of NWs in this environment, together with the high cost of conducting polymers themselves, have hindered applications of Ag NW-polymer composite TCFs [27, 28]. Drawbacks of graphene films include the current expensive fabrication procedures that use vacuum and high temperature steps together with time-consuming and complex multiple transfer steps from metal to Ag NWs networks [29]. Numerous grain boundaries in the graphene also increase its resistance, making it difficult to create high-quality graphene layers on a large scale [17].

On the basis of the above considerations, here, we report composite structures with a network of Ag NWs and reduced graphene oxide (r-GO). The GO solution was directly spin-coated onto the predeposited Ag NW networks. This composite film was coated by solution processes, which enabled cost-effective and high-speed fabrication of optoelectronic devices. We also introduced an auxiliary pressure step to weld the Ag NW networks during annealing at 100°C. Compared with other coating materials, such as metal oxides, GO with flake morphology could achieve the effect of full covering. Furthermore, the GO coating not only enhanced the antioxidant capacity of Ag NW networks but also could be reduced by ultraviolet light with the aid of the plasmonic Ag NWs as an auxiliary pathway in the composite film. These composite structures act as effective TCFs for potential applications as electrodes in devices with excellent optoelectronic performance [sheet resistance (Rs) ~ 7 ohm/sq and transparency (T) ~ 82% at λ = 550 nm] and environmental stability.

2. Materials and Methods

2.1. Preparation of Composite Films. The fabrication process of the Ag NW networks and r-GO composite films is schematically illustrated in Figure 1. First, Ag NWs with diameters in the range of 70-100 nm and lengths of 7-12 μm were dispersed in ethyl alcohol (~0.1 mg mL^{-1} suspension) and deposited on glass substrates by a drop-casting method. Then GO sheets with sizes of 500 nm were dispersed in aqueous solutions (~0.1 mg mL^{-1} suspension) and drop-coated onto the predeposited Ag NW networks. The Ag NWs and GO sheets were purchased from Nanjing XFNANO Material Tech Co., Ltd. Random Ag NW networks and GO composite films required a treatment at 100°C under pressure for 30 min in air to improve the electrical connections between wires. The composite film was placed on a heater and covered by a polytetrafluoroethylene plate, onto which different weights were placed to achieve the effect of a hot-press treatment at 100°C. The Ag NWs/GO composite films were exposed to a mercury lamp for 30 min. This method reduced the GO at room temperature owing to interactions of the UV light and Ag NW plasmons.

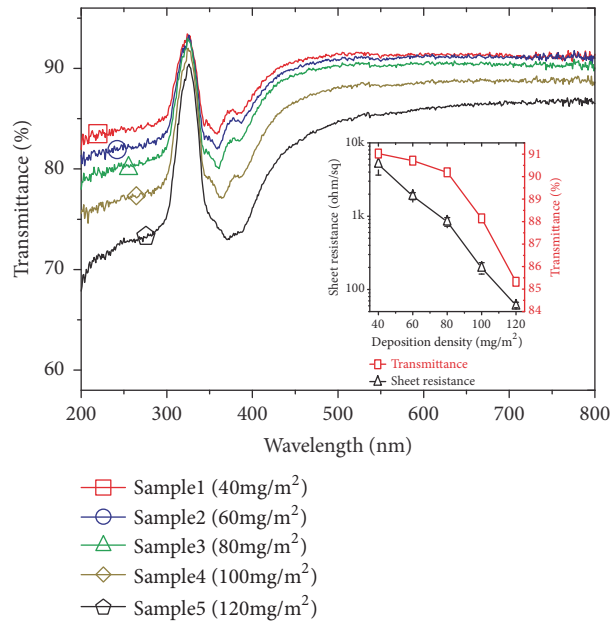

Figure 2: Optical transmittance spectra of the pure Ag NW networks under various densities; the inset shows the sheet resistance and transmission variation of pure Ag NW networks.

2.2. Characterization. The microstructures of the Ag NW networks and Ag NWs/r-GO composite films were characterized with a field emission scanning electron microscope (SEM, JSM-7610F). The transmittance spectra were measured on a UV/VIS spectrophotometer (Shimadzu UV-2600). The sheet resistance of the films was measured by the four-probe technique with a Keithley 6220 precision current source and a Keithley 2182A nanovoltmeter. Raman spectra of GO and Ag NWs/GO composite films were measured by Raman spectroscopy (Horiba Labram HR Evolution).

3. Results and Discussion

The optical properties of Ag NW networks were determined by measuring their transmittance spectra. Good optoelectronic performance is an important parameter for transparent electrodes. The transmittances of the pure Ag NW networks with NW densities from 40 to 120 mg/m^2 are shown in Figure 2. The transparency of the Ag NW network decreased as its density increased. The value of Rs decreased as the number of conductive pathways increased owing to the increased densities. The random networks of Ag NWs with different NW densities featured respective optical transmission (at 550 nm) and Rs values of 91.0% and 5084 ohm/sq (Sample 1), T ~ 90.7% and Rs ~ 1883.8 ohm/sq (Sample 2), T ~ 90.2% and Rs ~ 841 ohm/sq (Sample 3), T ~ 88.1% and Rs ~ 196 ohm/sq (Sample 4), and T ~ 85.3% and Rs ~ 61 ohm/sq (Sample 5), as shown in the inset of Figure 2. The Ag NW networks were highly transparent across all measured

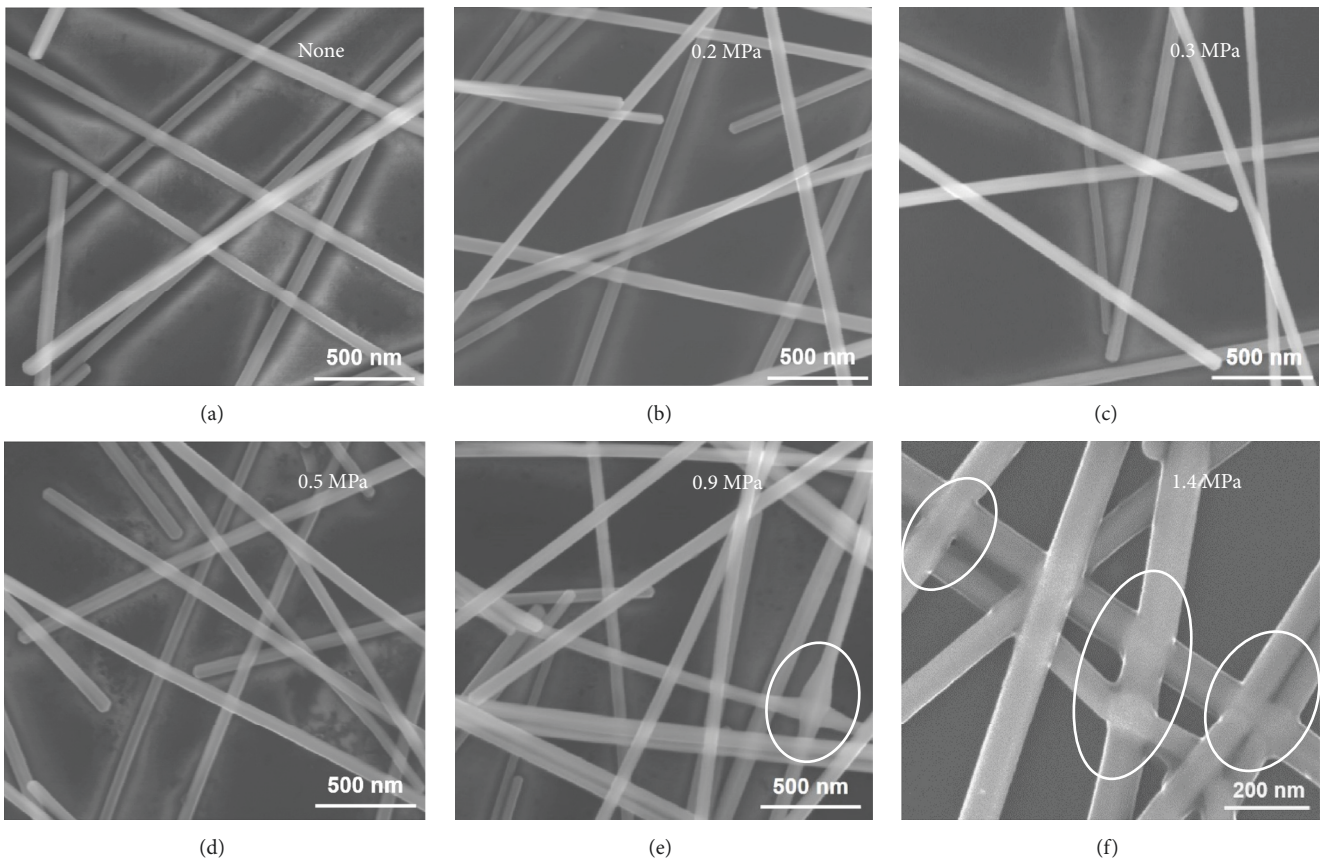

Figure 3: (a)-(f) SEM images of Ag NWs networks without (a) and at 0.2 (b), 0.3 (c), 0.5 (d), 0.9 (e), and 1.4 MPa (f) hot-pressing treatments at 100°C for 30 min.

wavelength regions because transmission in the mesh of random metallic nanowires was controlled almost entirely by the sparseness of the network, unlike ITO films that have absorptions from their band gap and from free electrons. To meet the high transmittance requirements of TCFs, for further studies we selected Sample 3, with a transmittance greater than 90% at 550 nm and 80 mg/m^2 deposition density.

Because the pristine Ag NWs were connected by the effects of gravity and weak van de Waals forces, the Rs of the Ag NW networks was greater than 800 ohm/sq owing to their small contact area. Furthermore, the bonding of the Ag NWs to the substrate was too weak to survive any further processing. Therefore, we proposed a hot-pressing method with a pressure applied at 100°C for 30 min in air to reduce the contact resistance and strengthen the bonding of the Ag NWs. An SEM image of the Ag NW networks after 30 min annealing at 100°C without pressure (Figure 3(a)) shows the small contact area at the cross-positions between NWs. The surface morphologies of the Ag NW networks annealed under pressures of 0.2, 0.3, 0.5, 0.9, and 1.4 MPa are shown in Figures 3(b)–3(f), respectively. As shown in Figure 3(e), a small amount of Ag NWs melted and fused together at crossing points under the hot-pressing conditions of 0.9 MPa. Figure 3(f) shows good welding at the cross-positions of Ag NWs after 1.4 MPa pressing.

To compare the electrical properties of the pure Ag NW networks before and after hot-pressing treatments, we plotted the effects of pressure and time on the Rs of the networks (Figure 4). The variation of Rs with increasing pressure in the range from 0 to 1.4 MPa for the pure Ag NW networks at 100°C for 30 min in air are shown in Figure 4(a). After this process, the Rs of the Ag NW networks decreased gradually from 445 to 32 ohm/sq, which is consistent with the good welding shown in the SEM image (Figure 3(f)). Full details of the hot-pressing time of the pure Ag NW network treated at 1.4 MPa and 100°C are shown in Figure 4(b). The lowest Rs (26 ohm/sq) was achieved at 30 min. The Ag NWs melted and broke into isolated Ag droplets at 40 min (SEM image shown in the inset of Figure 4(b)). Therefore, the conductivity of the Ag NW films was optimally improved by performing the hot-pressing treatment at 1.4 MPa and 100°C for 30 min.

To resolve the instability of the pure Ag NW networks in their environment, we proposed a method for fabricating Ag NWs/GO composite films. An SEM image (Figure 5(a)) indicated that GO sheets were deposited onto the pristine Ag NW networks by a drop-casting method. As shown in the TEM image (Figure 5(b)), multiple layers of GO flakes were superimposed on each other on top of the Ag NW networks. Then we performed the hot-pressing treatment immediately after covering the GO sheets according to the

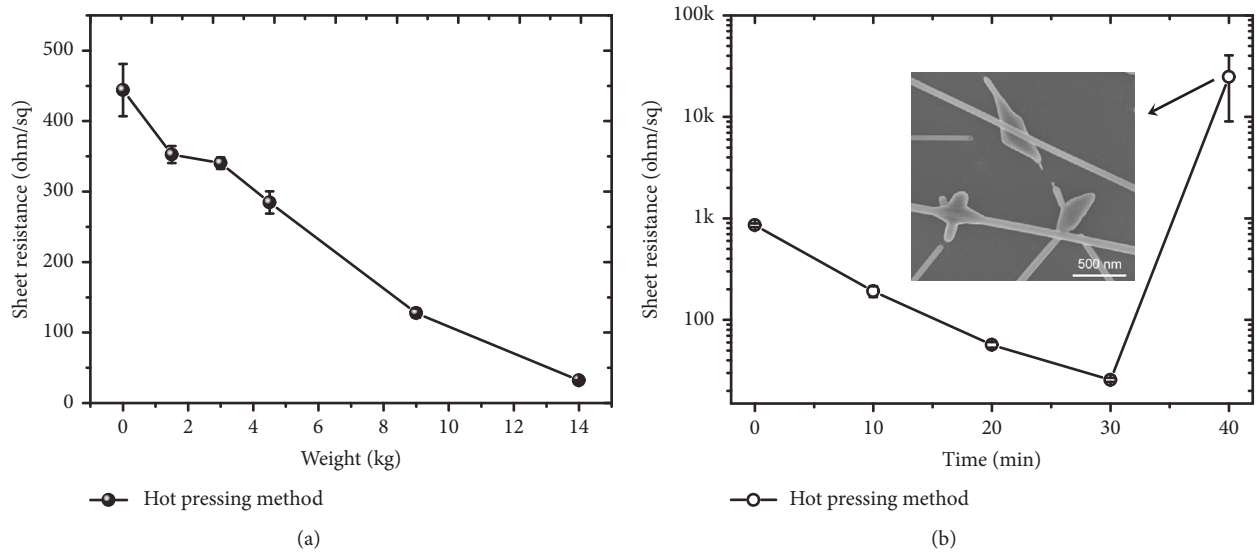

Figure 4: Variation of the sheet resistance of Ag NW networks under various pressures (a) and annealing temperatures (b); the inset shows an SEM image of the Ag NW networks under a hot-pressing treatment for 40 min.

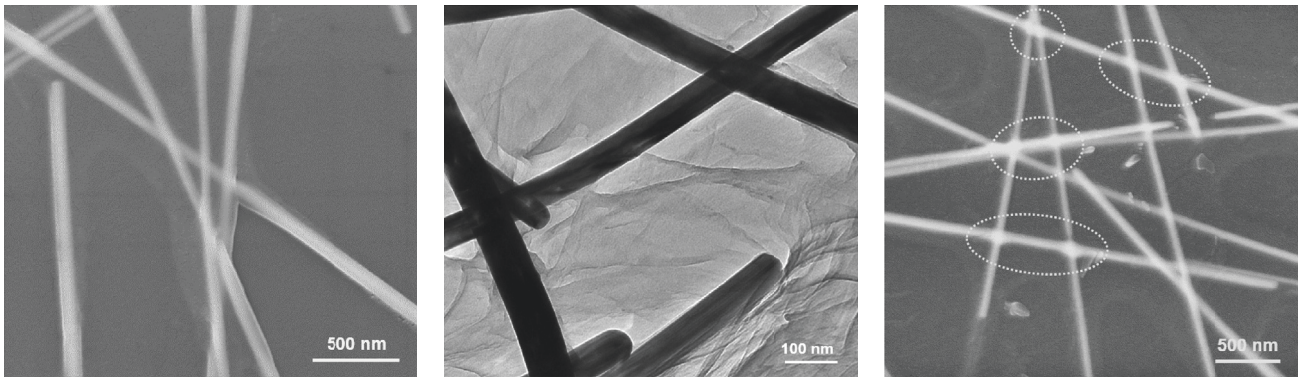

Figure 5: SEM image (a) and TEM image (b) of Ag NWs/GO composite films without treatments and SEM image of composite film treated by hot pressing (c).

optimal conditions. As shown in Figure 5(c), the Ag NWs melted and fused together at crossing points under the hot-pressing method under the protection of GO sheets. To become effective for commercial devices, Ag NW networks also require toughness and oxidation resistance.

To further improve the conductivity of the Ag NWs/GO composite films, the GO coatings were reduced by an efficient method. Using a nanoparticle plasmon-assisted and light-induced method, proposed by Lim and his coworkers [30], we reduced the GO. The absorption spectrum of the Ag NWs was measured to determine the resonance energy of localized surface plasmons. As shown in Figure 6(a), an extinction peak was centred at ~361 nm. Therefore, we performed the reaction using a mercury lamp (main excitation wavelength: 365 nm, power density: 30 MW cm^{-2}) to reduce the GO coatings and further reduce the Rs of the composite films. To confirm the quality of r-GO produced by the Ag NW plasmon-assisted method, we show the normalized Raman spectra of GO sheets and UV-irradiated GO sheets without or with Ag NW networks in Figure 6(b). In the Raman spectra of GO, the D band corresponding to the edge planes and disordered structures and the G band corresponding to ordered sp^2 bonded carbon appeared at 1327 and 1590 cm^{-1}, respectively [31, 32]. Therefore, the G/D intensity ratios (I_G/I_D) of GO and r-GO represent the number of defects in C atomic crystals and the degree of reduction of the GO coatings. The I_G/I_D of GO sheets and UV-irradiated GO without and with Ag NW networks were 0.95, 1.01, and 1.05, respectively. These results indicate that the quality of the r-GO prepared from the UV-treated plasmonic Ag NWs was better than that of the UV treatment alone. The weak power density of the mercury lamp and the multiple layers of GO

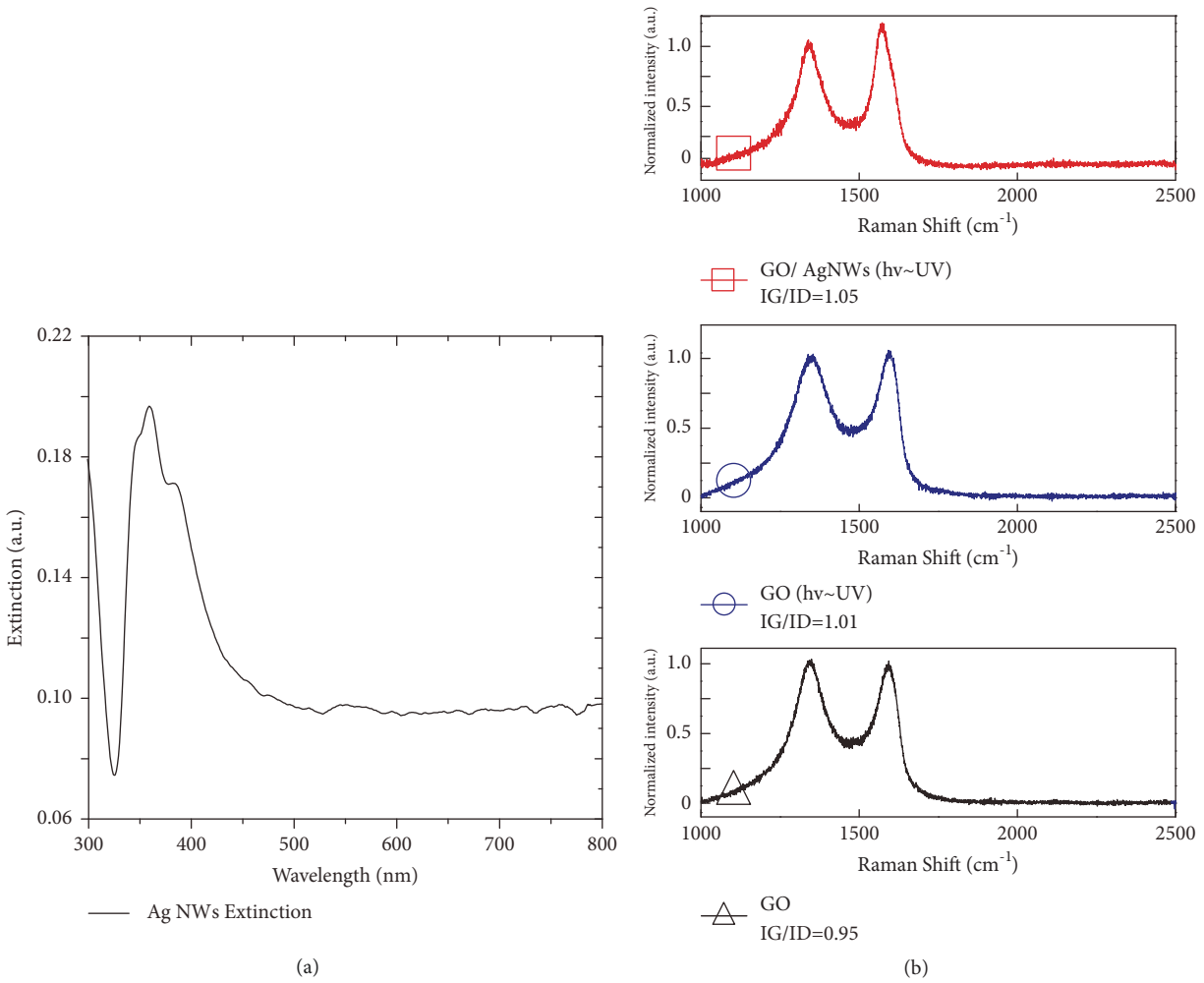

FIGURE 6: (a) Extinction spectrum of Ag NWs and (b) normalized Raman spectra of GO, GO after UV irradiation, and GO after UV irradiation with Ag NW plasmons.

flakes superimposed on the Ag NW networks might explain the relatively small change in the I_G/I_D values of GO sheets and UV-irradiated GO without or with Ag NW networks.

To verify the transmission properties of the Ag NWs/r-GO composite films, we measured transmission spectra of the Ag NW networks before and after covering with GO sheets without and with UV light-induced treatments which are shown in Figure 7(a). The transmittance of 86% (@ 550 nm) in the visible range of the Ag NW networks decreased owing to the involvement of the GO coatings. The transmittance of 82% at 550 nm for the composite films decreased after UV irradiation owing to the gradual recovery of the sp^2 conjugate structures in the r-GO sheets. In addition, we plot the Rs values of the pure Ag NW network and Ag NWs/GO composite films, which were reduced and unreduced in Figure 7(b). For the pure Ag NW network, the formation of silver oxide on the surface of the Ag NWs increased the resistance among the Ag NWs, which resulted in an increase of Rs in the Ag NW network. The Rs markedly increased from 23 to 246 ohm/sq after two months. By contrast, both GO and r-GO acted as a conformal passivation layer that protected the Ag NWs from oxidation. The GO coatings on the Ag NW networks further strengthened the contact between the NWs due to the capillary force caused by evaporation of the GO aqueous solution and the gravity of GO flakes, such that the Rs of the Ag NW/GO composite films decreased to 9.3 ohm/sq. After the UV treatment, the lattice defects and oxygen functional groups on the surface of the GO coatings were reduced. The r-GO coatings filled the empty regions in the Ag NW meshes. Although the resistance of r-GO was much larger than that of the Ag NW network, it acted as an auxiliary electron transport pathway in the composite films, resulting in the lowest Rs of 7 ohm/sq for the Ag NWs/r-GO composite film. The transmittance and the conductivity are typically inversely correlated attributes in these devices. The T value at 550 nm and the Rs were used to calculate a figure-of-merit Φ_{TE} for the transparent conducting electrodes, as defined by Haacke [33].

$$\Phi_{TE} = \frac{T^{10}}{Rs} \quad (1)$$

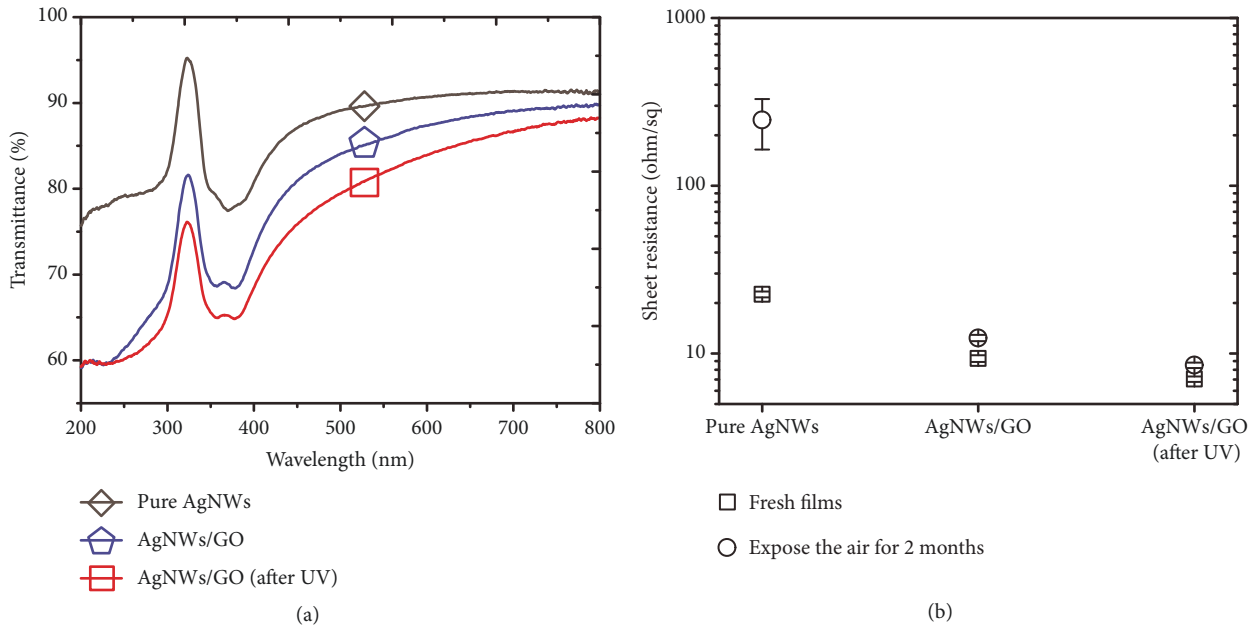

FIGURE 7: (a) Optical transmittance spectra of the pure Ag NW networks and the Ag NWs/GO composite film before and after UV light-induced treatment. (b) Environmental stability test of pure Ag NW networks and composite films.

The value Φ_{TE} of our Ag NW/GO composite film (19.64×10^{-3} ohm^{-1}, T ~ 82%, and Rs ~ 7 ohm/sq) is higher than the value based on a TCF deposited from a traditional material (i.e., ITO, 11.62×10^{-3} ohm^{-1}, T ~ 90%, and Rs ~ 30 ohm/sq). The Rs value increased by only 1.5 ohm/sq after two months. Stability to oxidation is an important factor for application of Ag NWs-based TCFs.

4. Conclusions

In conclusion, we propose a composite structure based on a network of Ag NWs with an r-GO coating to realize high-performance transparent conductors. We hot-pressed the Ag NW networks to decrease the Rs value (approximately 32 times) of the Ag NW networks without sacrificing transparency. Furthermore, the Ag NWs acted as plasmonic NWs to assist in UV irradiation-induced reduction of GO sheets, which made the r-GO coatings an additional electron transport pathway and improved the conductivity of the Ag NWs/r-GO composite film. A minimum Rs of 7 ohm/sq with 82% transmittance at 550 nm was obtained in this composite film. Furthermore, our composite structure showed good stability in air with a stable Rs of 8.5 ohm/sq after two months.

Data Availability

The readers can login to the following URL to access the data underlying the findings of the study: https://pan.baidu.com/s/1lriTUia2L4sjAc7vtI1euA. Code: 4yuu.

Conflicts of Interest

The authors declare that there are no conflicts of interest regarding the publication of this paper.

Acknowledgments

This work is supported by the National Natural Science Foundation of China (no. 51672103), National Key R&D Program of Strategic Advanced Electronic Materials of China (no. 2016YFB0401103), and the Science and Technology Development Project of Jilin Province, China (nos. 20160204069GX, 20170101111JC, 20170520169JH, 20180520227JH, JJKH20180589KJ, and JJKH20170243KJ).

References

[1] G. Haacke, "Transparent conducting coatings," *Annual Review of Materials Research*, vol. 7, pp. 73–93, 1977.

[2] R. G. Gordon, "Criteria for choosing transparent conductors," *MRS Bulletin*, vol. 25, no. 8, pp. 52–57, 2000.

[3] Z. C. Wu, Z. H. Chen, X. Du et al., "Transparent, conductive carbon nanotube films," *Science*, vol. 305, no. 5688, pp. 1273–1276, 2004.

[4] P. B. Catrysse and S. Fan, "Nanopatterned metallic films for use as transparent conductive electrodes in optoelectronic devices," *Nano Letters*, vol. 10, no. 8, pp. 2944–2949, 2010.

[5] P. Kuang, J.-M. Park, W. Leung et al., "A new architecture for transparent electrodes: relieving the trade-off between electrical conductivity and optical transmittance," *Advanced Materials*, vol. 23, no. 21, pp. 2469–2473, 2011.

[6] Y. Leterrier, L. Médico, F. Demarco et al., "Mechanical integrity of transparent conductive oxide films for flexible polymer-based displays," *Thin Solid Films*, vol. 460, no. 1-2, pp. 156–166, 2004.

[7] M. Kang, M. Kim, J. Kim, and L. J. Guo, "Organic solar cells using nanoimprinted transparent metal electrodes," *Advanced Materials*, vol. 20, no. 23, pp. 4408–4413, 2008.

[8] K. Tvingstedt and O. Inganäs, "Electrode grids for ITO-free organic photovoltaic devices," *Advanced Materials*, vol. 19, no. 19, pp. 2893–2897, 2007.

[9] J. Lee, S. T. Connor, Y. Cui, and P. Peumans, "Solution-processed metal nanowire mesh transparent electrodes," *Nano Letters*, vol. 8, no. 2, pp. 689–692, 2008.

[10] S. De, T. M. Higgins, P. E. Lyons et al., "Silver nanowire networks as flexible, transparent, conducting films: extremely high DC to optical conductivity ratios," *ACS Nano*, vol. 3, no. 7, pp. 1767–1774, 2009.

[11] L. Hu, H. S. Kim, J.-Y. Lee, P. Peumans, and Y. Cui, "Scalable coating and properties of transparent, flexible, silver nanowire electrodes," *ACS Nano*, vol. 4, no. 5, pp. 2955–2963, 2010.

[12] X. Yan, J. Ma, H. Xu, C. Wang, and Y. Liu, "Fabrication of silver nanowires and metal oxide composite transparent electrodes and their application in UV light-emitting diodes," *Journal of Physics D: Applied Physics*, vol. 49, no. 32, p. 325103, 2016.

[13] M. Zhang, S. Fang, A. A. Zakhidov et al., "Materials science: strong, transparent, multifunctional, carbon nanotube sheets," *Science*, vol. 309, no. 5738, pp. 1215–1219, 2005.

[14] M. W. Rowell, M. A. Topinka, and M. D. McGehee, "Organic solar cells with carbon nanotube network electrodes," *Applied Physics Letters*, vol. 88, no. 23, Article ID 233506, 2006.

[15] X. Wang, L. J. Zhi, and K. Mullen, "Transparent, conductive graphene electrodes for dye-sensitized solar cells," *Nano Letters*, vol. 8, no. 1, pp. 323–327, 2008.

[16] H. A. Becerril, J. Mao, Z. Liu, R. M. Stoltenberg, Z. Bao, and Y. Chen, "Evaluation of solution-processed reduced graphene oxide films as transparent conductors," *ACS Nano*, vol. 2, no. 3, pp. 463–470, 2008.

[17] J. Wu, M. Agrawal, H. A. Becerril et al., "Organic light-emitting diodes on solution-processed graphene transparent electrodes," *ACS Nano*, vol. 4, no. 1, pp. 43–48, 2010.

[18] D. Azulai, T. Belenkova, H. Gilon, Z. Barkay, and G. Markovich, "Transparent metal nanowire thin films prepared in mesostructured templates," *Nano Letters*, vol. 9, no. 12, pp. 4246–4249, 2009.

[19] A. Kumar and C. Zhou, "The race to replace tin-doped indium oxide: which material will win?" *ACS Nano*, vol. 4, no. 1, pp. 11–14, 2010.

[20] A. Kim, Y. Won, K. Woo, S. Jeong, and J. Moon, "All-solution-processed indium-free transparent composite electrodes based on Ag nanowire and metal oxide for thin-film solar cells," *Advanced Functional Materials*, vol. 24, no. 17, pp. 2462–2471, 2014.

[21] Y. Wu, J. Xiang, C. Yang, W. Lu, and C. M. Lieber, "Single-crystal metallic nanowires and metal/semiconductor nanowire heterostructures," *Nature*, vol. 430, no. 6995, pp. 61–65, 2004.

[22] L. Yang, T. Zhang, H. Zhou, S. C. Price, B. J. Wiley, and W. You, "Solution-processed flexible polymer solar cells with silver nanowire electrodes," *ACS Applied Materials & Interfaces*, vol. 3, no. 10, pp. 4075–4084, 2011.

[23] W. Hu, X. Niu, L. Li, S. Yun, Z. Yu, and Q. Pei, "Intrinsically stretchable transparent electrodes based on silver-nanowire-crosslinked-polyacrylate composites," *Nanotechnology*, vol. 23, no. 34, 2012.

[24] L. Hu, H. Wu, and Y. Cui, "Metal nanogrids, nanowires, and nanofibers for transparent electrodes," *MRS Bulletin*, vol. 36, no. 10, pp. 760–765, 2011.

[25] W. Gaynor, G. F. Burkhard, M. D. McGehee, and P. Peumans, "Smooth nanowire/polymer composite transparent electrodes," *Advanced Materials*, vol. 23, no. 26, pp. 2905–2910, 2011.

[26] D. Y. Choi, H. W. Kang, H. J. Sung, and S. S. Kim, "Annealing-free, flexible silver nanowire-polymer composite electrodes via a continuous two-step spray-coating method," *Nanoscale*, vol. 5, no. 3, pp. 977–983, 2013.

[27] E. Voroshazi, B. Verreet, T. Aernouts, and P. Heremans, "Long-term operational lifetime and degradation analysis of P3HT: PCBM photovoltaic cells," *Solar Energy Materials & Solar Cells*, vol. 95, no. 5, pp. 1303–1307, 2011.

[28] M. Jørgensen, K. Norrman, S. A. Gevorgyan, T. Tromholt, B. Andreasen, and F. C. Krebs, "Stability of polymer solar cells," *Advanced Materials*, vol. 24, no. 5, pp. 580–612, 2012.

[29] I. N. Kholmanov, M. D. Stoller, J. Edgeworth et al., "Nanostructured hybrid transparent conductive films with antibacterial properties," *ACS Nano*, vol. 6, no. 6, pp. 5157–5163, 2012.

[30] D. Kumar, S. Kaur, and D.-K. Lim, "Plasmon-assisted and visible-light induced graphene oxide reduction and efficient fluorescence quenching," *Chemical Communications*, vol. 50, no. 88, pp. 13481–13484, 2014.

[31] A. C. Ferrari and J. Robertson, "Interpretation of Raman spectra of disordered and amorphous carbon," *Physical Review B: Condensed Matter and Materials Physics*, vol. 61, no. 20, pp. 14095–14107, 2000.

[32] F. Tuinstra and J. L. Koenig, "Raman spectrum of graphite," *The Journal of Chemical Physics*, vol. 53, no. 3, pp. 1126–1130, 1970.

[33] G. Haacke, "New figure of merit for transparent conductors," *Journal of Applied Physics*, vol. 47, no. 9, pp. 4086–4089, 1976.